Supporting Information for

Activation of NF-κB signalling by fusicoccin-induced dimerization

Authors: Malgorzata Skwarczynska[1], Manuela Molzan[1] and Christian Ottmann[1,2]

Affiliations:

[1]Chemical Genomics Centre of the Max-Planck-Society, Otto-Hahn-Str. 15, 44227 Dortmund, Germany

[2]Laboratory of Chemical Biology, Department of Biomedical Engineering, Technische Universiteit Eindhoven, Den Dolech, 5612 AZ Eindhoven (The Netherlands)

Corresponding author: e-mail: christian.ottmann@cgc.mpg.de, c.ottmann@tue.nl

Supporting Methods.

SupportingResults.

Supporting References.

Supporting Methods.

DNA construction and PCR-based mutagenesis. The cDNA templates of *Nicotiana tabaccum* T14-3-3c (NCBI accession number U91724), *Nicotiana plumbaginifolia* PMA2 (NCBI accession number M27888), human 14-3-3 isoforms β, ε, η, γ, σ, τ and ζ (NCBI accession numbers BC001359, BC001440, NM_003405, BC020963, BC000329, NM_006826, BC083508) and human Cdc25A (NCBI accession number NM_001789) were purchased from Open Biosystems Inc. For T14-3-3cΔC (residues1-242), a PCR product encoding *N. tabaccum* T14-3-3c was subcloned into the expression vector pProEx-HTb (Invitrogen) by the use of primers with restriction sites for BamHI and SalI. Full-length human 14-3-3 cDNA were subcloned into the same expression vector through the restriction sites BamHI and SalI (β, ε, η, γ, ζ) or BamHI and NotI (σ, τ), respectively. The expression vector pQE30 (Qiagen) described in our previous work (1) containing full-length cDNA of *N. tabaccum* T14-3-3c and a C-terminal GFP, was used to express His_6 tagged T14-3-3c-GFP for surface-based fluorescence assay. The GST expression vector pGEX4-T-1 containing the C-terminus of *N. plumbaginifolia* PMA2 CT66 (residues 891-956) and the expression vector pTYB12 containing CT52 (residues 905-956) are described in our previous work (2, 3). Site directed mutagenesis of all T14-3-3c and PMA2 constructs were performed by using the QuikChange™ Site-Directed Mutagenesis Kit (Agilent technologies). The primers used for site-directed mutagenesis were: PMA2-K943D: Forward primer: 5'-CGAATCAGTGGTGAAGTTGGACGGTCTTGACATAGAGACAA-3', Reverse primer: 5'-TTGTCTCTATGTCAAGACCGTCCAACTTCACCACTGATTCG-3'; PMA2-K943E: Forward primer: 5'-GAATCAGTGGTGAAGTTGGAGGGTCTTGACATAGAGA-3', Reverse primer: 5'-TCTCTATGTCAAGACCCTCCAACTTCACCACTGATTC-3'; PMA2-S938A: Forward primer: 5'-TGAAAGGTCACGTCGAAGCAGTGGTGAAGTTGGA-3', Reverse primer: 5'-TCCAACTTCACCACTGCTTCGACGTGACCTTTCA-3'; PMA2-

T955D-V956I-pGex: Forward primer: 5'-AGACAATTCAGCAATCATACGATATTTGAG-TCGACTCGAGCGGCC-3', Reverse primer: 5'-GGCCGCTCGAGTCGACTCAAATATC-GTATGATTGCTGAATTGTCT-3'; PMA2-T955D-V956I-pTYB12: Forward primer: 5'-G-ACAATTCAGCAATCATACGATATTTGAGTCGACGGCGGC-3', Reverse primer:5'-G-CCGCCGTCGACTCAAATATCGTATGATTGCTGAATTGTC-3'; T14-3-3c-E19R: Forward primer: 5'-AACGTGTACATGGCAAAGCTTGCAAGGCAAGCTGAGAGG-3', Reverse primer: 5'-CCTCTCAGCTTGCCTTGCAAGCTTTGCCATGTACACGTT-3'; T14-3-3c-E19K: Forward primer: 5'-ACGTGTACATGGCAAAGCTTGCAAAGCAAGCT-GAGA-3', Reverse primer: 5'-TCTCAGCTTGCTTTGCAAGCTTTGCCATGTACACGT-3'; T14-3-3c-Y137F: Forward primer: 5'-AGGAGATTACCACCGCTTTTTGGCTGAGTT-CAAGA-3', Reverse primer: 5'-TCTTGAACTCAGCCAAAAAGCGGTGGTAATCTCCT. For life imaging studies PCR products encoding T14-3-3cΔC-M1/M2, were cut with NheI and XhoI and with ApaI und BamHI and were subcloned into the mammalian expression vector pEGFP-N1 (Clontech). Additionally further PCR products encoding T14-3-3cΔC-M1/M2, were digested with BspEI und XhoI and with BamHI und XbaI and were inserted into pEGFP-C1 (Clontech). PCR products encoding CT52M1, were cut with BamHI and XbaI and inserted into the mammalian expression vector pmCherry-C1 (Clontech). For pEGFP-N1-T14-3-3cΔC-M2-NLS a nuclear localization signal from human Cdc25A (residues 268-297) was digested with SacII and SmaI and subcloned into pEGFP-N1-T14-3-3cΔC-M2 digested with the same set of restriction enzymes. For pmCherry-N-Myr-CT52M1 primers encoding a plasma membrane targeting signal (Forward primer: 5'-CTAGCGATGGGGAGTAGCAAGAGCAAGCCTAAGGACCCCAGCCAGCGCGGA-3', Reverse primer: 5'-CCGGTCCGCGCTGGCTGGGGTCCTTAGGCTTGCTCTTGCTACTC-CCCATCG) were annealed, digested with NheI and AgeI and subcloned into pmCherry-CT52M1. Forp65-CT52M1 full-length human p65 was amplified from p65-dsRed-XP, which was a gift of Prof. Michael R. H. White, cut with HindIII and KpnI and

subcloned into pmCherry-CT52M1. The cloning of p65, p65-CT52M1 and T14-3-3cΔC-M2-NLS into the vector pOPIN-NHis was performed by the Dortmund Protein Facility. All cloning and mutated constructs were verified by sequencing.

Protein expression and purification. Protein expression in *E. coli* Rosetta (DE3) of all His_6 tagged 14-3-3 proteins, as well as GST-CT66 and CT52 variants was induced by addition of 0.4 mM IPTG at 20 ºC for 12 h. Purification of all His_6 tagged 14-3-3 proteins was carried out using Ni-NTA-Sepharose (Qiagen), whereas purification of all GST fusion proteins was carried out using GSH-Sepharose (Amersham Pharmacia Biotech) according to the manufacturer's protocol. Proteins were concentrated to 40-80 mg/ml and dialyzed against 20 mMHepes/NaOH pH 7.5, 2 mM $MgCl_2$ and 0.5 mM TCEP. CT52 variants were expressed as intein fusion peptides and isolated without its fusion protein according to the manufacturer's instructions (IMPACT-CN, New England Biolabs). The CT52 peptides were concentrated to ~5 mg/ml and dialyzed against 20 mM Hepes/NaOH pH 7.5, 100 mM NaCl, 2 mM $MgCl_2$ and 0.5 mM TCEP. Recombinant protein purity was estimated to be >95% by Coomassie staining. All protein variants were snap frozen in liquid nitrogen and stored at -80°C.

Surface-based fluorescence assay. The measurements were carried out at 25 °C essentially as described in our previous work(1). Briefly, a 0.02 µg/µl solution of each GST-CT66 variant in 25 mM Tris/HCl pH 7.5, 150 mM NaCl, 2 mM $MgCl_2$ (SBF buffer) was immobilized for 2 h at room temperature in a flat bottom polystyrene high binding 96-well microplate in a volume of 100 µl per well. Wells were blocked with 100 µl of SBF + 0.05% Tween20 and 1% BSA (w/v) for 1 h at room temperature followed by three washing steps with 100 µl of SBF + 0.05% Tween20. Subsequently wells were incubated overnight at 4 °C with 100 µl SBF containing 0.02 µg/µl T14-3-3c-GFP variants and 3 µM FC. On the following day three

washing steps were performed as described before and GFP fluorescence was measured at 485 nm using the Infinite®F500 plate reader (Tecan).

Cell Fractioning and Western Blotting. HEK293T cells were cultured as described above. 5×10^5 cells per well were plated in 6-well plates in 2 ml medium and grown for 24 hours prior to co-transfection, which was carried as described above with plasmids encoding mCherry-fused p65-CT52M1 and GFP-fused T14-3-3cΔC-M2-NLS. 24 hours post transfection cells were treated with 5 µM FC and incubated for another 16 hours before fractioning. Cell fractioning was performed using the ProteoExtract® Subcellular Proteom Extraction Kit (Calbiochem). For cells treated with FC a concentration of 5 µM FC was maintained in all washing and extraction buffers. Samples of the nuclear fractions were mixed with 100µl 5x-SDS-sample buffer, 30µl of the resulting mixture separated on a 15 % SDS-PAGE gel and transferred to a Nitrocellulose membrane. Non-specific sites were blocked as described above. mCherry-fused p65-CT52 was detected by a mouse monoclonal anti-mCherry antibody (Abcam) used at 1:2000 in 5% milk in TBS-T. As a loading control an anti-Histone H3 antibody (Millipore) was used at a concentration of 1:500. Both antibodies were detected by an anti-mouse antibody derived from goat coupled to AP (Cell Signaling) at a dilution of 1:1000.

SupportingResults.

^{891}HGLQVPDTKLFSEATNFNELNQLAEEAKRRAEIARQRELHTLKGHVESVVKLKGLDIETIQQSYTV^{956}-COOH

^{891}HGLQVPDTKLFSEATNFNELNQLAEEAKRRAEIARQRELHTL**K**GHVE**A**VVKLKGLDIETIQQSY**DI**^{956}-COOH

Fig. S1. Sequence of the regulatory C-terminus of *N. plumbaginifolia* plasma membrane H^+-ATPase PMA2. The sequence below shows the amino acid substitutions (bold and underlined) that led to an enhanced binding to tobacco T14-3-3cΔC (S938A, T955D and V956I) (3). This construct served as positive control in this study. The K943 we chose for protein engineering in this study is underlined. The schematic representation of the CT66 and CT52 constructs is displayed below.

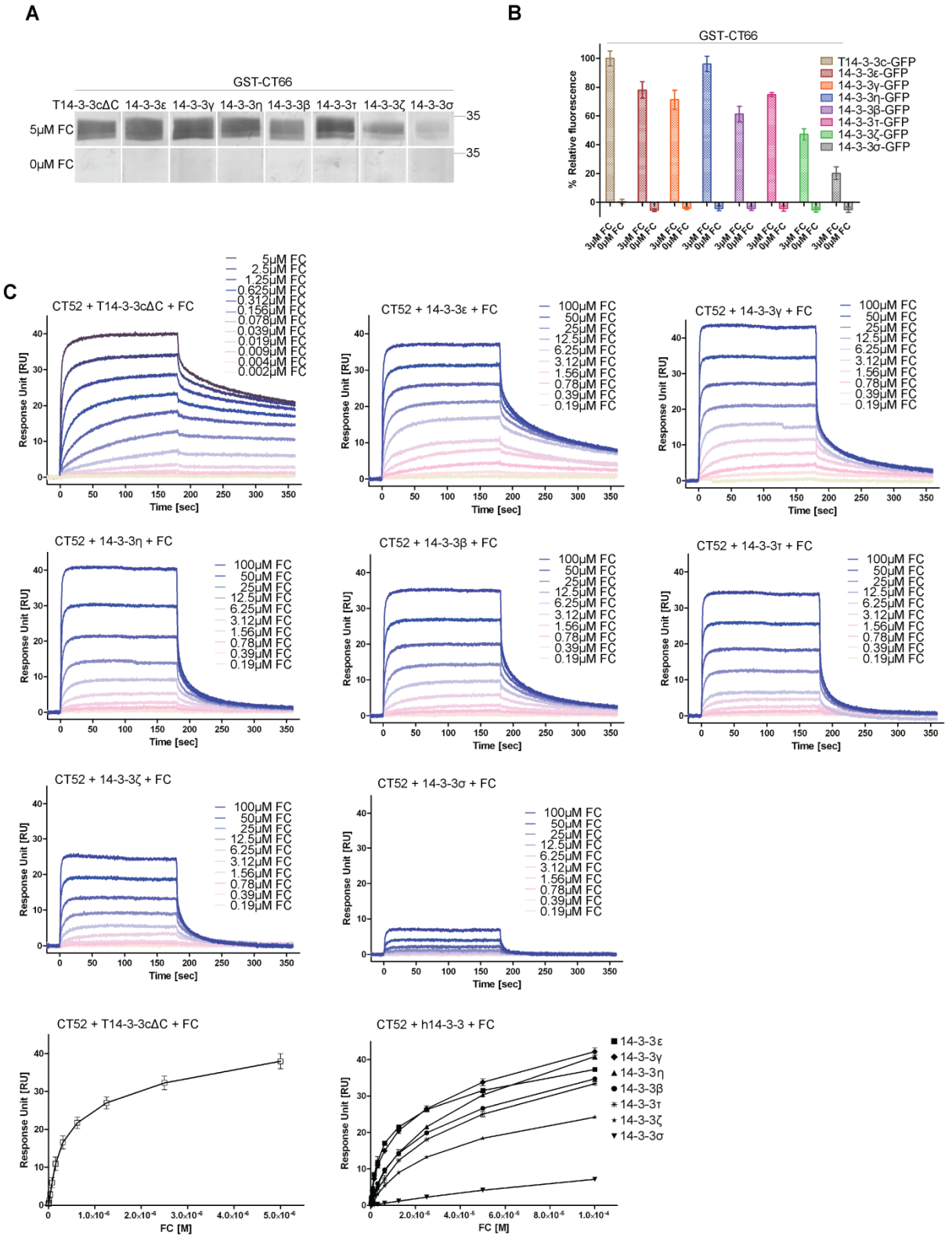

Fig. S2. Interaction of PMA-Peptide (CT66/CT52) and wild type 14-3-3 proteins. (*A*) Binding of T14-3-3cΔC and human 14-3-3 isoforms to immobilized GST-CT66 was measured in presence and absence of 5 μM FC by Far-Western blotting. (*B*) Surface-based fluorescence measurements of GST-CT66 to T14-3-3cΔCWt and human 14-3-3 isoforms (β, ε, η, γ, σ, τ and ζ). Results (bar graph) are mean ± s.e.m of three independent experiments, n=6. (*C*) SPR measurements performed to calculate the EC_{50} values of FC on the CT52/14-3-3 interaction.

Here FC was titrated in presence of 10 μM T14-3-3cΔC or human 14-3-3 proteins (β, η, γ, σ, τ and ζ) stepwise in 1:1 dilutions onto immobilized CT52 until saturation was reached. The RU values were plotted against time or the corresponding FC concentration, respectively.

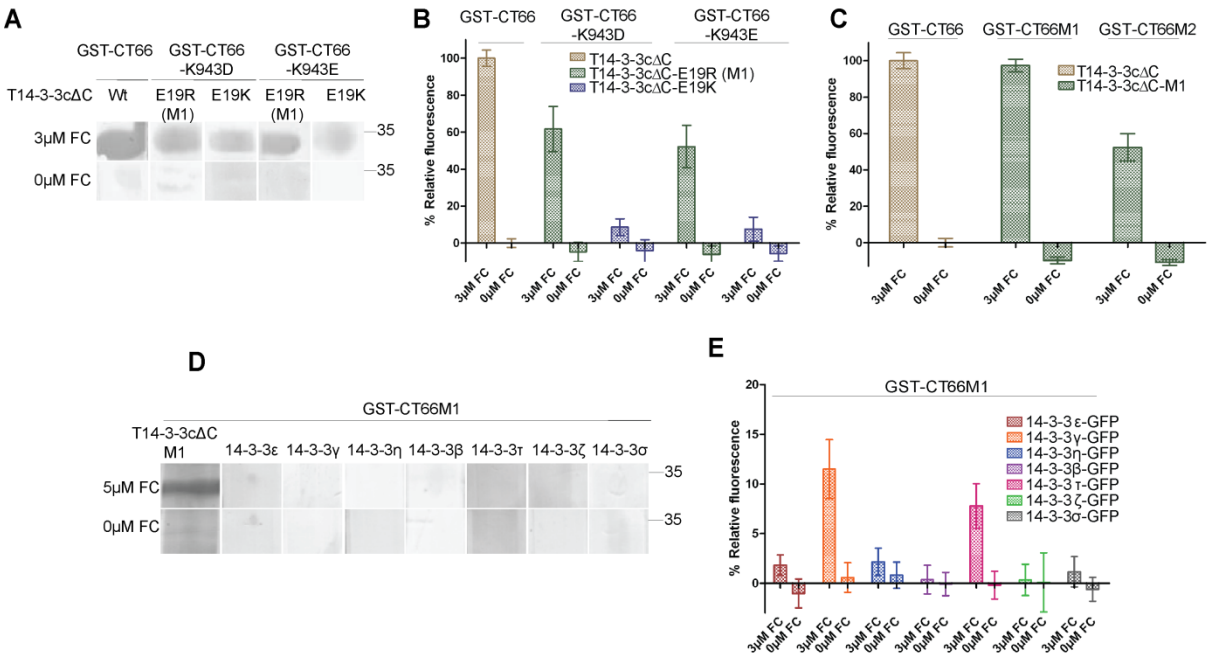

Fig. S3. Interaction of CT66 and T14-3-3cΔC variants. (*A*) Binding of GST-CT66, GST-CT66-K943D and GST-CT66-K943E toT14-3-3cΔC, T14-3-3cΔC-E19R (M1) and T14-3-3cΔC-E19K measured in presence and absence of 3 μM FC by Far-Western blotting. (*B-C*) Surface-based fluorescence measurements. Immobilized GST-CT66 variants were incubated for 16 hours with T14-3-3cΔC variants fused to GFP in presence and absence of 3 μM FC. Subsequently the GFP fluorescence was measured. Results (bar graph) are mean ± s.e.m of three independent experiments, n=6. (*B*) Binding of GST-CT66, GST-CT66-K943D and GST-CT66-K943E to T14-3-3cΔC, T14-3-3cΔC-E19R (M1) and T14-3-3cΔC-E19K. (*C*) Binding of GST-CT66, GST-CT66M1 and GST-CT66M2 to T14-3-3cΔC and T14-3-3cΔC-E19R (M1). (*D*) Binding of T14-3-3cΔC-M1 and human 14-3-3 to GST-CT66M1 was measured in presence and absence of 5 μM FC by Far-Western blotting. (*E*) Surface-based fluorescence measurements of GST-CT66M1 to human 14-3-3 proteins. Results (bar graph) are mean ± s.e.m of three independent experiments, n=6.

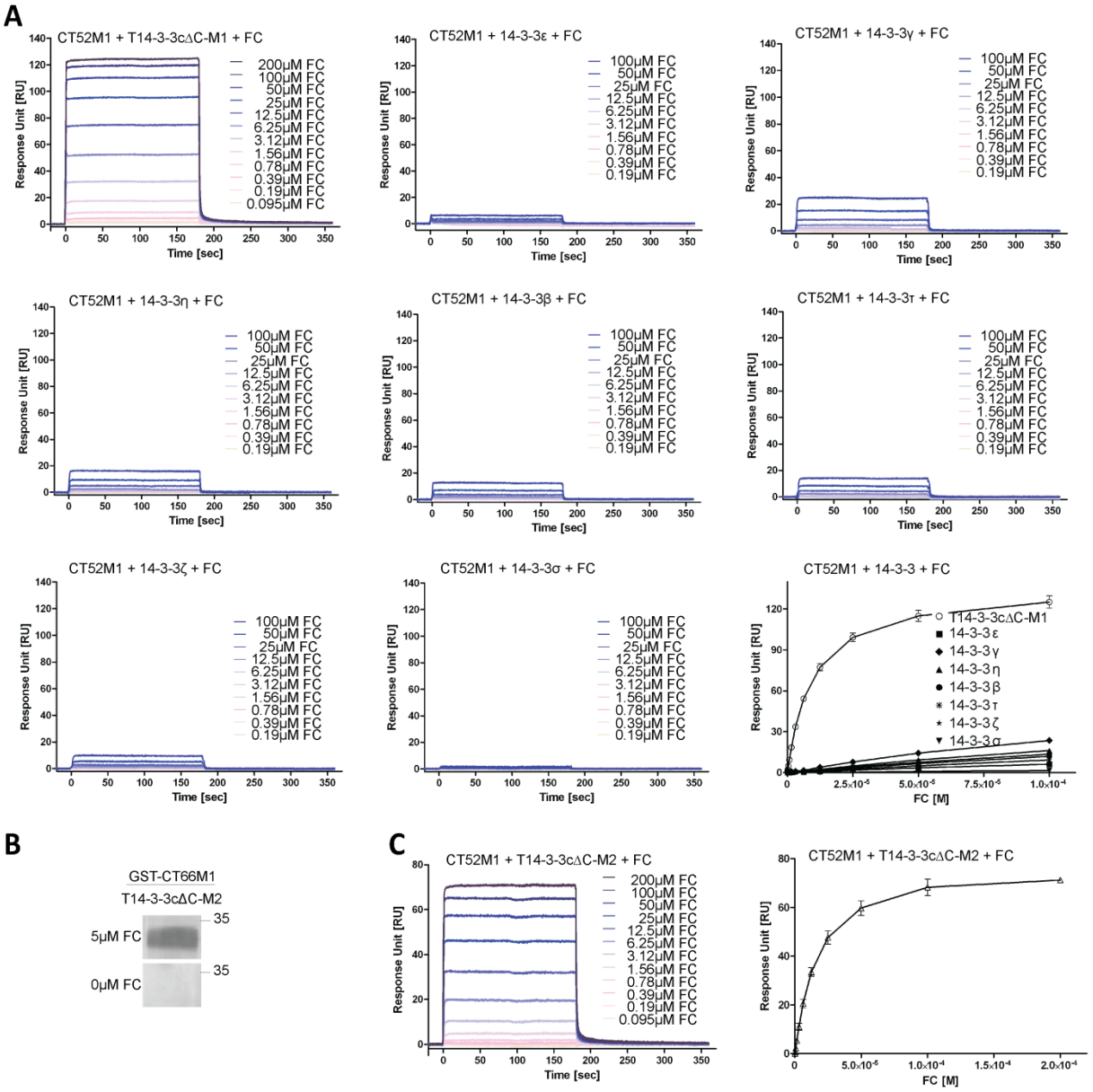

Fig. S4. Interaction of mutated PMA-Peptides (CT66M1/CT52M1) and T14-3-3cΔC variants and human 14-3-3 wild type proteins, respectively. (*A*) SPR measurements performed to calculate the EC_{50} values of FC on the CT52M1/14-3-3 complex. Here FC was titrated in presence of 10 µM 14-3-3 proteins (T14-3-3cΔC-M1, β, η, γ, σ, τ and ζ) stepwise in 1:1 dilutions onto immobilized CT52M1 until saturation was reached. The RU values were plotted against time or the corresponding FC concentration, respectively. (*B*) Far-Western blot analysis of GST-CT66M1 with T14-3-3cΔC-M2 in presence and absence of 5 µM FC. (*C*) SPR measurement of T14-3-3cΔC-M2 on CT52M1. FC was titrated in presence of 10 µM T14-3-3cΔC-M2 stepwise in 1:1 dilutions. The RU values were plotted against time or the corresponding FC concentration, respectively.

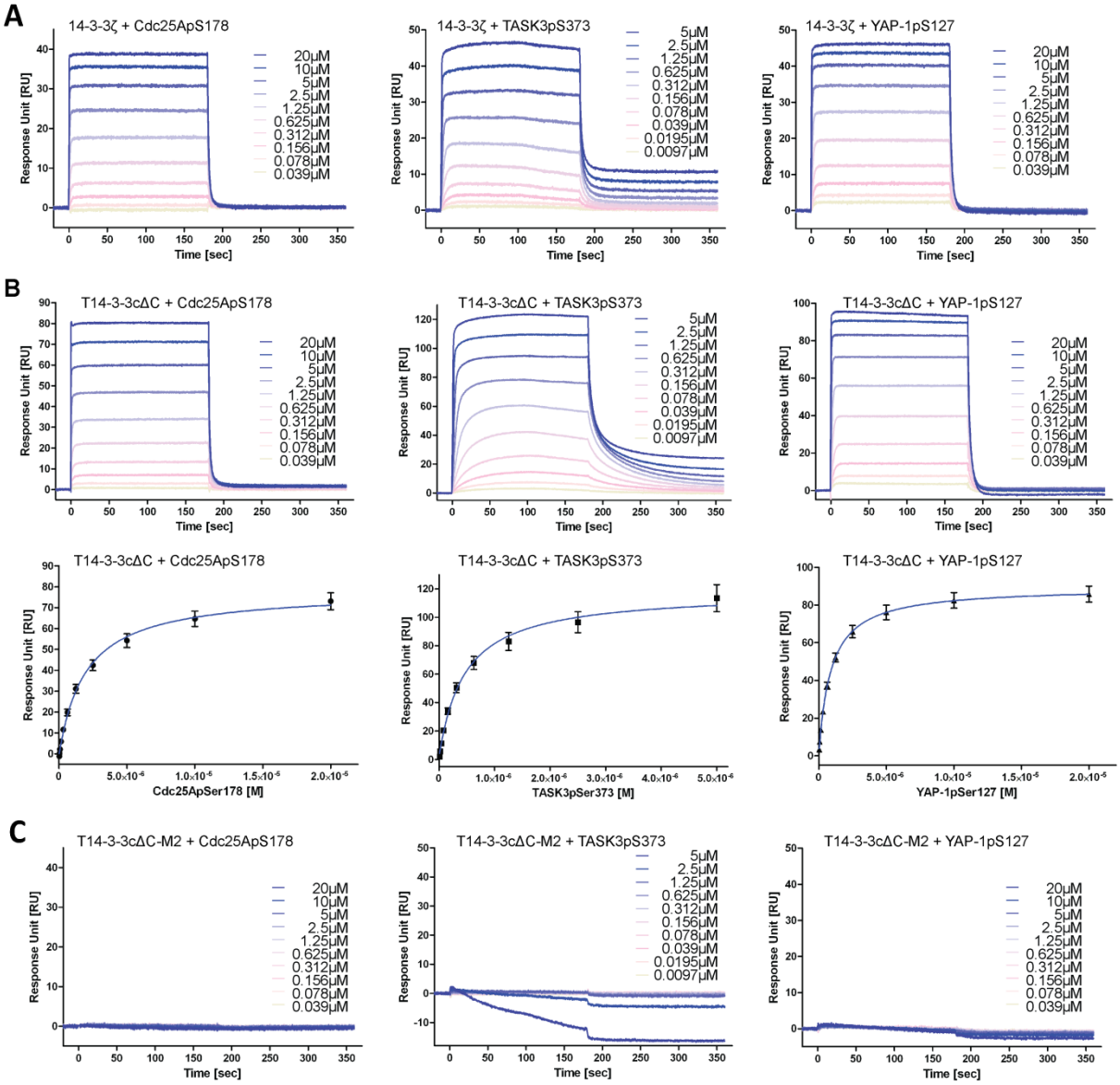

Fig. S5. SPR measurements of phosphopeptides containing the 14-3-3 binding motif of Cdc25A, TASK3 or YAP-1 to immobilized 14-3-3 proteins. (*A*) Binding affinity was measured by stepwise titration of the peptides in 1:1 dilutions onto 14-3-3ζ surface until reaching saturation. (*B*) Corresponding measurements onto immobilized T14-3-3cΔC. For the interaction of the phosphopeptides and T14-3-3cΔC the corresponding curves could be fitted using steady state kinetics (blue curves) and K_D values could be calculated (Table 2). (*C*) Corresponding measurements onto immobilized T14-3-3cΔC-M2.

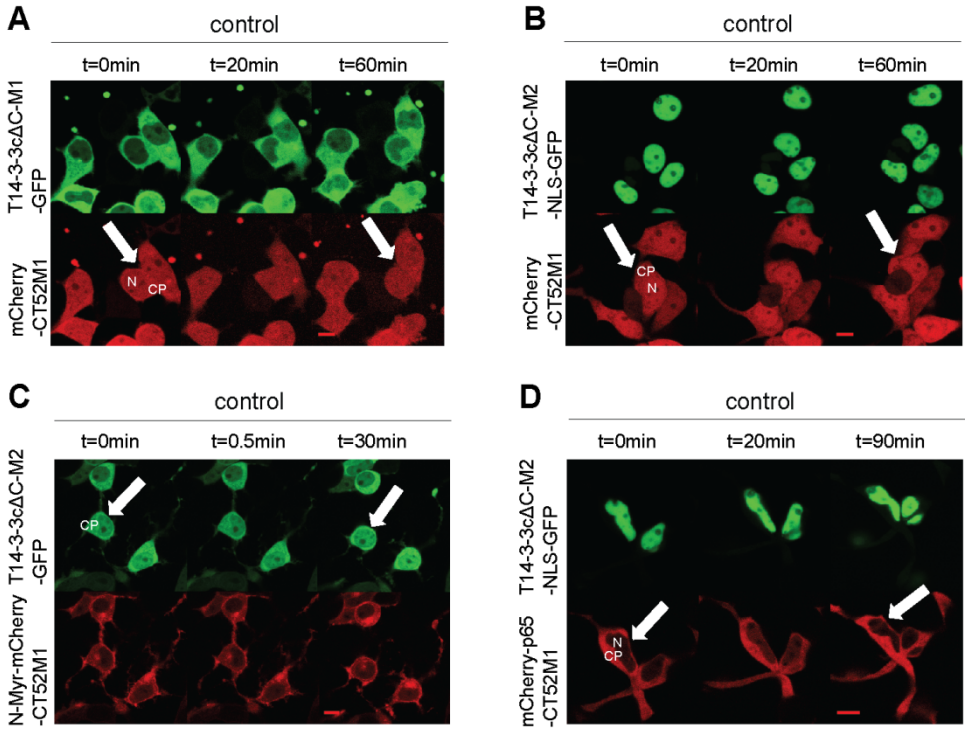

Fig. S6. Time course images of control cells. HEK293T co-transfected with the same plasmids used for nuclear exclusion, nuclear accumulation, plasma membrane recruitment and nuclear import of p65 (Fig. 3*B*, 4*A*, 4*C*, 5*B*) and treated with solvent (3.3% ethanol). Neither a translocation of mCherry-CT52M1 out of the nucleus or into the nucleus, nor a translocation of T14-3-3cΔC-M2-GFP to the plasma membrane, nor translocation of mCherry-p65-CT52M1 into the nucleus was observed. Scale bars, 10 µm, N: nucleus, CP: cytoplasm.

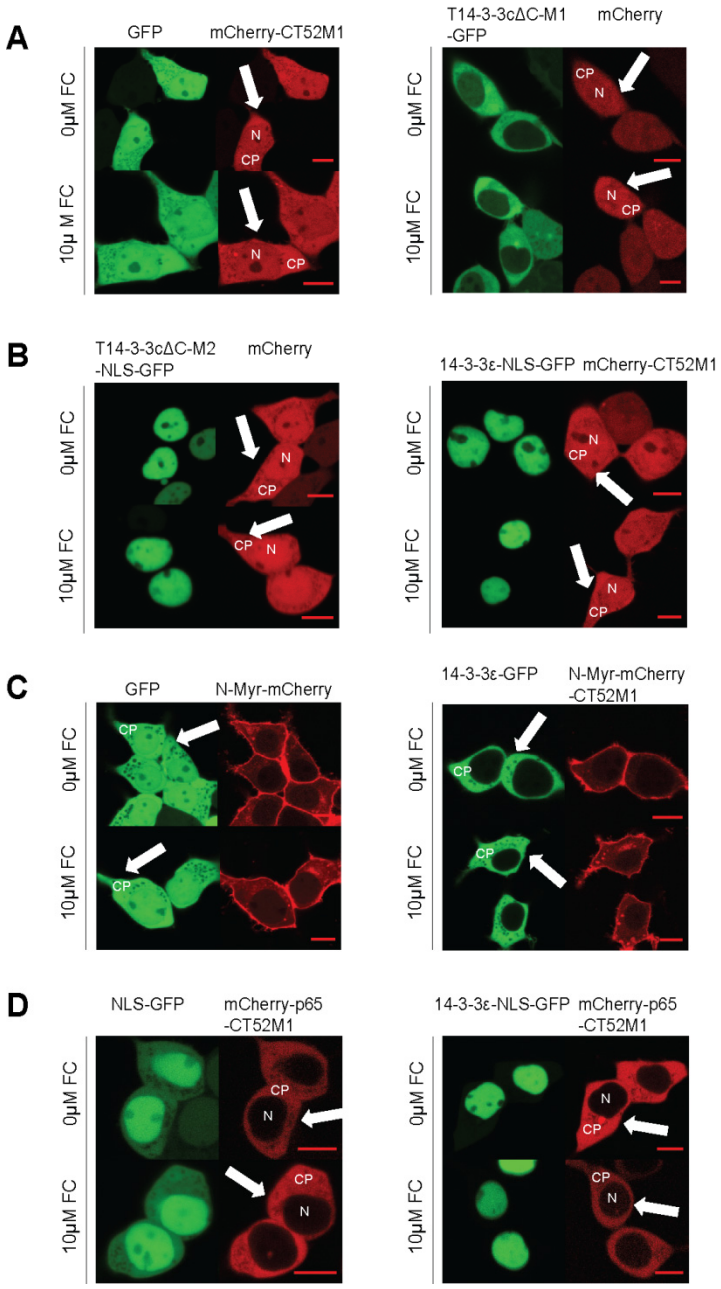

Fig. S7. Control experiments with constructs encoding for only one FC binding partner. For further control experiments HEK293T cells were co-transfected with plasmids encoding for corresponding GFP and mCherry constructs and were either untreated (each upper panel) or treated with 10 µM FC for 16 h (each lower panel). After treatment of the cells with FC a change of fluorescence intensities in the compartments was not observed (A-D). Scale bars, 10 µm, N: nucleus, CP: cytoplasm.

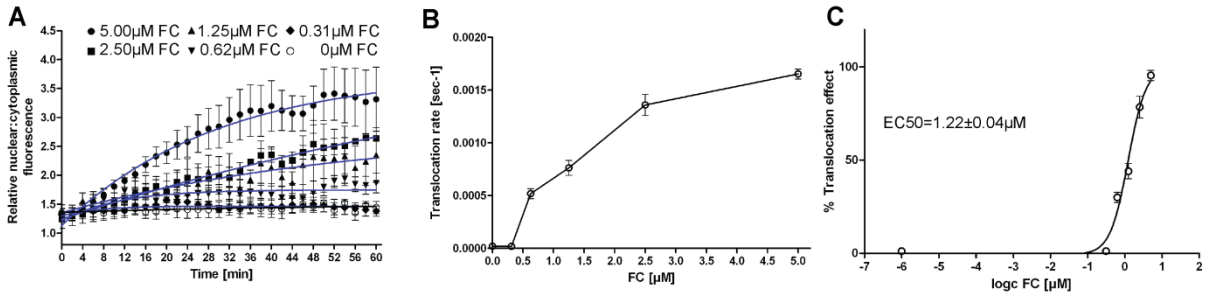

Fig. S8. Quantification of mCherry-CT52M1 translocation. (*A*) Measurements were performed in response to different FC concentrations, with co-transfected T14-3-3cΔC-M2-NLS-M2-GFP (as well as the analysis of untreated cells (control). Mean cytoplasmic and nuclear fluorescence intensities were calculated every 2 minutes and plotted as a ratio against time. (*B*-*C*) Determination of the nucleus membrane translocation rate to calculate the EC_{50} of FC. The curve was fitted using the four parameter logistic nonlinear regression model. The data represent mean values (±s.e.m.) from three experiments with at least two cells per experiment. These experiments were performed in HEK293T cells.

A

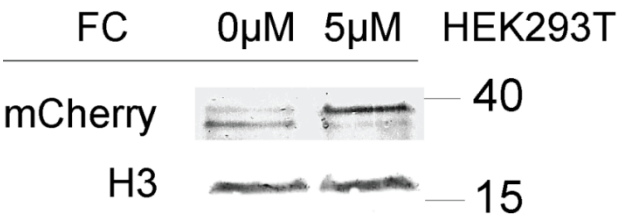

B

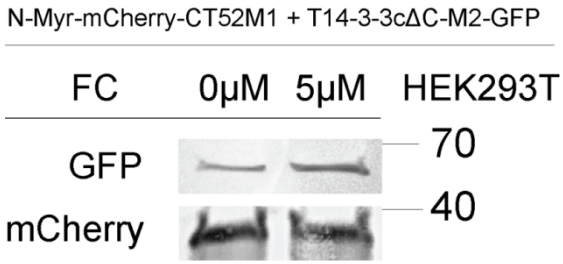

Fig. S9. (A) Nuclear accumulation of mCherry-CT52M1 in FC treated cells. HEK293T cells transfected with plasmids encoding for T14-3-3cΔC-NLS-GFP and mCherry-CT52M1 were treated with 0 µM and 5 µM FC. After cell fractioning the nuclear probe was analyzed by Western blotting using the anti-mCherry antibody. Anti-Histone H3 was used as nuclear marker. (B) Plasma membrane accumulation of T14-3-3cΔC-M2-GFP in FC treated cells. HEK293T cells transfected with plasmids encoding for N-Myr-mCherry-CT52M1 and T14-3-3cΔCM2-GFP were treated with 0 µM and 5 µM FC. After cell fractioning the plasma membrane probe was analyzed by Western blotting using an anti-GFP and a mCherry antibody.

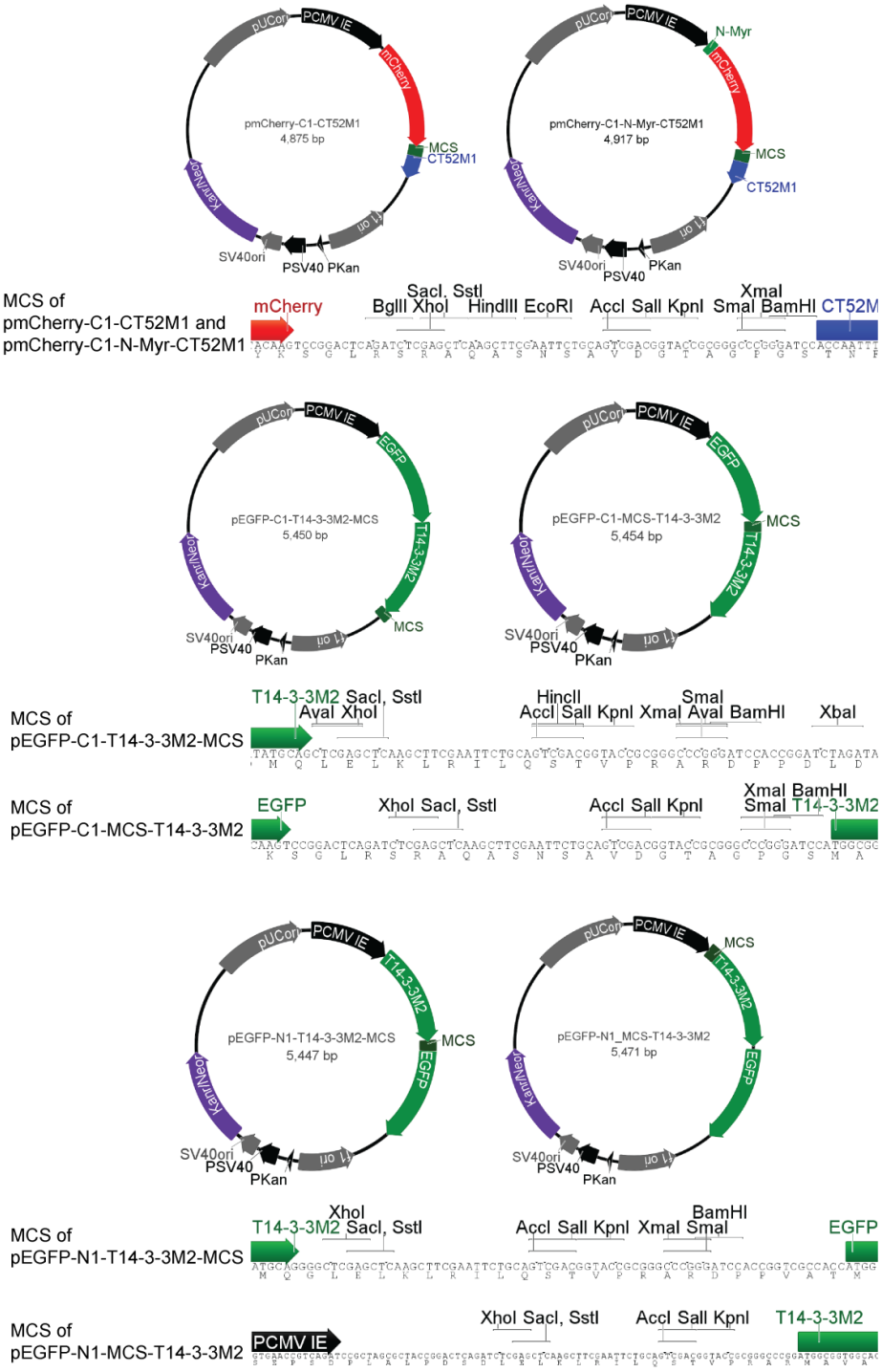

Fig. S10. Mammalian expression vectors created for this study. Modified pEGFP-C1, pEGFP-N1 and pmCherry-C1 contain the corresponding cDNA for the FC-binding proteins. The vectors each include a gene encoding for enhanced fluorescence proteins, either GFP or mCherry, allowing detection of the target protein by confocal microscopy. They also contain a multiple cloning site for inserting genes encoding for proteins of choice for an individual use of this CID system. pmCherry-C1-N-Myr-CT52M1 in addition contains a plasma membrane targeting signal. For more information about the vectors see also http://www.clontech.com. Plasmid maps were generated using Geneious Pro 5.3.6, available from http://www.geneious.com.

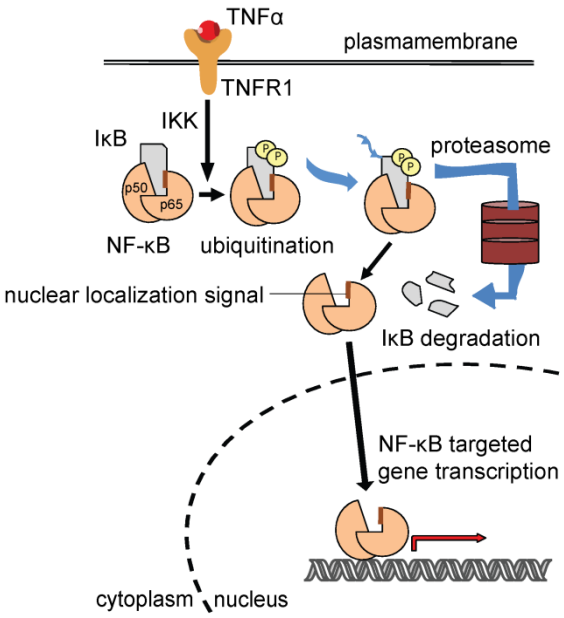

Fig. S11. TNFα induced nuclear accumulation of NF-κB. Simplified scheme of the NF-κB signaling pathway (modified from (5). Unphosphorylated IκB retains NF-κB by binding to the heterodimer (p50/p65). In TNFα stimulated cells IκB is phosphorylated by IKK and subsequently ubiquitinated, leading to its degradation. Thereby NF-κB`s NLS is exposed, inducing protein translocation into the nucleus where NF-κB dependent target gene transcription is induced.

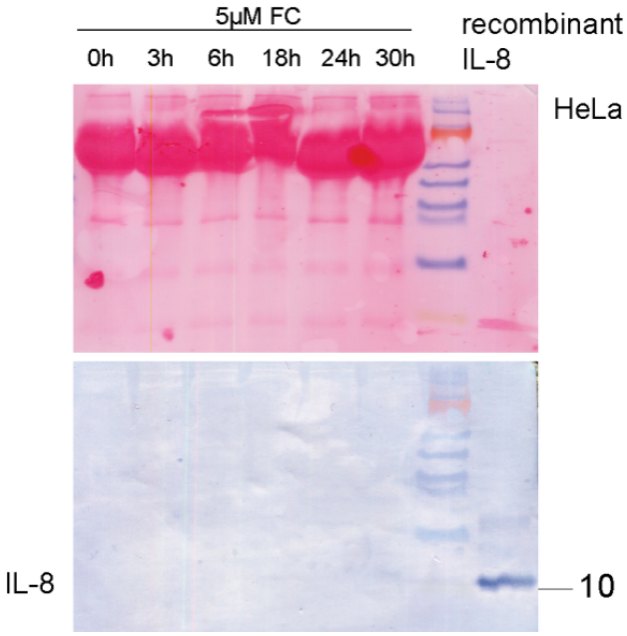

Fig. S12. FC treatment of untransfected HeLa cells. Untransfected HeLa cells treated with 5 µM FC were analyzed for IL-8 expression during a time course of 30 hours by Western blotting. IL-8 expression was not observed. For a positive control recombinant IL-8 was detected. Upper panel: Ponceau S stain, Lower panel: Western blot.

Table S1: Sequences of phosphorylated peptides used in this study.

Peptide name	Sequence
Cdc25ApS178	^{170}DLFTQRQN-pS-APARMLSSNERDSSEPGNFIPLFTPQSPV^{207}
YAP-1pS127	^{121}QHVRAH-pS-SPASLQLGAVSPGTLT^{143}
TASK3pS373	^{343}KNSLFPSPISSISPGLHSFTDHQRLMKRRK-pS-V^{374}

Table S2: Comparison of the most important CID systems. Regarding the ligand binding protein, only the fragment that binds the dimerizer is listed. CID systems containing ligands, that bind to endogenous FKBP, cyclophilin, FRAP, calcineurin or DHFR are highlighted in gray, while CID systems containing dimerizers that display no interferences to endogenous binding proteins are highlighted in orange (GyrB, bacterial DNA gyraseB; DHFR, dihydrofolate reductase).

dimerizer	description	ligand binding protein	ligand binding protein	size (kDa)	comment	reference
Homodimerizer						
FK1012	FK506 homodimer	FKBP (3 copies)	FKBP (3 copies)	12/12	interferences with endogenous FKBP	(6)
AP1510	homodimer derived from the synthetic ligand of FKBP (SLF, FK506-analog)	FKBP (3 copies)	FKBP (3 copies)	12/12	simpler molecule than FK1012, that allows modification; more stable than FK1012; interferences with endogenous FKBP	(7)
AP1903	modified („*bumped*") derivative of AP1510	FKBP- F36V (3 copies)	FKBP- F36V (3 copies)	12/12	no interferences with endogenous FKBP, non-toxic	(8)
coumermycin	substance obtained from Streptomyces	GyrB	GyrB	24/24	interferences with mammalian DHFR excluded	(9)
*bis*MTX	methotrexat homodimer	bacterial DHFR	mouse DHFR	18/18	interferences with endogenous DHFR, used only in cell free systems, nano-assembly	(10)
Heterodimerizer						
FK506	macrolide obtained from *S. tsukubaensis*	FKBP (3 copies)	calcineurin A (CnA)	12/58	interferences with endogenous FKBP and CnA, inhibits the CnA-mediated activation of NF-AT, binding to single components	(11)
FK506-derivative	C40-modified FK506	FKBP (3 copies)	mCAB (fusion of $CnA_{340-394}$ and CnB_{3-170} with specific mutations)	12/25	interferences with endogenous FKBP,	(12)
FKCsA	Dimer composed of FK506 and cyclosporin A (CsA, substance from *T. inflatum*)	FKBP (3 copies)	cyclophilin	12/21	interferences with endogenous FKBP and cyclophilin,	(13)
rapamycin	macrolide obtained from *S. hygroscopicus*	FKBP (3 copies)	FRB	12/11	interferences with endogenous FKBP and FRB, inactivates the endogenous FRAP-kinase, most common dimerizer,	(14)
rapalogs	synthetic rapamycin-derivatives; C16/C20-modified rapamycin	FKBP (3 copies)	FRB with specific mutations	12/11	interferences with endogenous FKBP,	(15, 16)
TMP-SLF	dimer composed of trimethoprim and synthetic ligand of FKBP (SLF, FK506-analog)	FKBP (3 copies)	bacterial DHFR	12/18	no interferences neither with human DHFR nor to endogenous calcineurin A; not excluded non-productive binding of SLF to FKBP; binding to single components	(17)
ABA	S-(+)-abscisic acid, plant hormone from higher plants	PYL_{CS}	ABI_{CS}	20/33	no interferences with mammalian endogenous proteins, non-toxic,	(18)
GA_3-AM	cell-permeable gibberellin-analog, plant hormone from higher plants	GID1	GAI	38/10	no interferences with mammalian endogenous proteins;	(19)
FC	plant toxin from *P. amygdali*	T14-3-3cΔC-M2	PMA2-CT52M1	27/6.5	no interferences with mammalian endogenous proteins; binds only to the binary complex;	this study

Supporting Movies Descriptions

SV1. nuclear exclusion_5µM FC.avi

Here mCherry-CT52M1 is co-transfected with T14-3-3cΔC-M1-GFP. T14-3-3cΔC-M1-GFP is localized in the cytoplasm, while mCherry-CT52M1 shuttles between the cytoplasm and nucleus. After addition of 5µM FC to the HEK293T cells mCherry-CT52M1 is forming a complex with T14-3-3cΔC-M1-GFP, thereby trafficking into the cytoplasm. Time-frame: 60 minutes.

SV2. nuclear exclusion_revers.avi

Here the reversibility of the nuclear excluded mCherry-CT52M1 is demonstrated by rinsing the cells with FC-free medium. The ternary complex of mCherry-CT52M1, T14-3-3cΔC-M1-GFP and FC dissociates, so that part of the cytoplasmic population of mCherry-CT52M1 is trafficking back into the nucleus. Time-frame: 60 minutes.

SV3. nuclear accumulation_5µM FC.avi

Here mCherry-CT52M1 is co-transfected with T14-3-3cΔC-M2-NLS-GFP. T14-3-3cΔC-M2-NLS-GFP is localized in the nucleus, while mCherry-CT52M1 shuttles between the cytoplasm and nucleus. After addition of 5µM FC to the HEK293T cells mCherry-CT52M1 is forming a complex with T14-3-3cΔC-M2-NLS-GFP and is thereby translocated into the nucleus. Time-frame: 60 minutes.

SV4. nuclear accumulation_revers.avi

Here the reversibility of the nuclear accumulated mCherry-CT52M1 is demonstrated by rinsing the cells with FC-free medium. The ternary complex of mCherry-CT52M1, T14-3-3cΔC-M2-NLS-GFP and FC dissociates, so that part of the nuclear population of mCherry-CT52M1 is trafficking back into the cytoplasm. Time-frame: 60 minutes.

SV5. pm recruitment_5µM FC.avi

Here N-Myr-mCherry-CT52M1 is co-transfected with T14-3-3cΔC-M2-GFP. T14-3-3cΔC-M2-GFP shuttles between nucleus and cytoplasm, while N-Myr-mCherry-CT52M1 is recruited to the plasma membrane. After addition of 5µM FC to the HEK293T cells T14-3-3cΔC-M2-GFP is forming a complex with N-Myr-mCherry-CT52M1 and is thereby recruited within few seconds to the plasma membrane. Time-frame: 30 minutes.

SV6. pm recruitment_revers FC.avi

Here the reversibility of the plasma membrane recruited T14-3-3cΔC-M2-GFP is demonstrated by rinsing the cells with FC-free medium. The ternary complex of N-Myr-mCherry-CT52M1, T14-3-3cΔC-M2-GFP and FC dissociates, allowing translocation of T14-3-3cΔC-M2-GFP back into the cytoplasm and nucleus. Time-frame: 30 minutes.

SV7. p65 nuclear import_5μM FC.avi

Here mCherry-p65-CT52M1 is co-transfected with T14-3-3cΔC-M2-NLS-GFP. T14-3-3cΔC-M2-NLS-GFP is localized in the nucleus, while mCherry-p65-CT52M1 is localized in the cytoplasm. After addition of 5μM FC to the HEK293T cells mCherry-p65-CT52M1 is forming a complex with T14-3-3cΔC-M2-NLS-GFP and is thereby translocated into the nucleus. Time-frame: 90 minutes.

SV8. p65 nuclear import_revers FC.avi

Here the reversibility of the nuclear accumulated mCherry-p65-CT52M1 is demonstrated by rinsing the cells with FC-free medium. The ternary complex of mCherry-p65-CT52M1, T14-3-3cΔC-M2-NLS-GFP and FC dissociates, so that part of the nuclear population of mCherry-p65-CT52M1 is trafficking back into the cytoplasm. Time-frame: 80 minutes.

Supporting References

1. Rose R et al. (2010) Identification and structure of small-molecule stabilizers of 14-3-3 protein-protein interactions. *Angew. Chem. Int. Ed. Engl.* 49:4129-4132.

2. Jelich-Ottmann C, Weiler EW, Oecking C (2001) Binding of regulatory 14-3-3 proteins to the C terminus of the plant plasma membrane H^+-ATPase involves part of its autoinhibitory region. *J. Biol. Chem.* 276:39852-39857.

3. Ottmann C et al. (2007) Structure of a 14-3-3 coordinated hexamer of the plant plasma membrane H^+-ATPase by combining X-ray crystallography and electron cryomicroscopy. *Mol. Cell* 25:427-440.

4. Wu JT, Kral JG (2005) The NF-κB/IκB signaling system: a molecular target in breast cancer therapy. *J Surg Res* 123:158-169.

5. Gilmore TD (1999) The Rel/NF-κB signal transduction pathway: introduction. *Oncogene* 18:6842-6844.

6. Spencer DM, Wandless TJ, Schreiber SL, Crabtree GR (1993) Controlling signal transduction with synthetic ligands. *Science* 262:1019-1024.

7. Amara JF et al. (1997) A versatile synthetic dimerizer for the regulation of protein-protein interactions. *Proc. Natl. Acad. Sci. USA* 94:10618-10623.

8. Clackson T et al. (1998) Redesigning an FKBP-ligand interface to generate chemical dimerizers with novel specificity. *Proc. Natl. Acad. Sci. USA* 95:10437-10442.

9. Farrar M, Alberola-Lla J, Permutter R (1996) Activation of the Raf-1 kinase cascade by coumermycin-induced dimerization. *Nature* 383:178-181.

10. Kopytek SJ, Standaert RF, Dyer JC, Hu JC (2000) Chemically induced dimerization of dihydrofolate reductase by a homobifunctional dimer of methotrexate. *Chemistry & biology* 7:313-21.

11. Ho SN, Biggar SR, Spencer DM, Schreiber SL, Crabtree GR (1996) Dimeric ligands define a role for transcriptional activation domains in reinitiation. *Nature* 382:822-826.

12. Clemons P a et al. (2002) Synthesis of calcineurin-resistant derivatives of FK506 and selection of compensatory receptors. *Chem. Biol.* 9:49-61.

13. Belshaw P, Ho S, Crabtree G, Schreiber S (1996) Controlling protein association and subcellular localization with a synthetic ligand that induces heterodimerization of proteins. *Proc. Natl. Acad. Sci. USA* 93:4604-4607.

14. Rivera V et al. (1996) A humanized system for pharmacologic control of gene expression. *Nat. Med.* 2:1028-1032.

15. Liberles SD, Diver ST, Austin DJ, Schreiber SL (1997) Inducible gene expression and protein translocation using nontoxic ligands identified by a mammalian three-hybrid screen. *Proc. Natl. Acad. Sci. USA* 94:7825-7830.

16. Bayle JH et al. (2006) Rapamycin analogs with differential binding specificity permit orthogonal control of protein activity. *Chem. Biol.* 13:99-107.

17. Czlapinski J et al. (2008) Conditional glycosylation in eukaryotic cells using a biocompatible chemical inducer of dimerization. *J. Am. Chem. Soc.* 130:13186-13187.

18. Liang F-S, Ho WQ, Crabtree GR (2011) Engineering the ABA plant stress pathway for regulation of induced proximity. *Sci. Signal.* 4:rs2.

19. Miyamoto T et al. (2012) Rapid and orthogonal logic gating with a gibberellin-induced dimerization system. *Nat. Chem. Biol.*:1-6.